
Proceedings Paper:
Foster, RJ orcid.org/0000-0002-5337-3615, Hine, PJ, Bonner, MJ et al. (1 more author) (2008) The incorporation of carbon nanofibres to enhance the properties of hot compacted self-reinforced single polymer composites. In: Proceedings of the 13th European Conference on Composite Materials (ECCM 13). ECCM 13: The 13th European Conference on Composite Materials, 02-05 Jun 2008, Stockholm, Sweden. European Society for Composite Materials .

THE INCORPORATION OF CARBON NANOFIBRES TO ENHANCE THE PROPERTIES OF HOT COMPACTED SELF-REINFORCED SINGLE POLYMER COMPOSITES

Richard J Foster [1,2], Peter J Hine [1,2], Mark J Bonner [1] and Ian M Ward [1,2]

[1] *IRC in Polymer Science & Technology, Polymer & Complex Fluids Group, School of Physics & Astronomy*

[2] *Nanomanufacturing Institute, School of Process, Environmental & Materials Engineering*

University of Leeds, Leeds, UK, LS2 9JT

Corresponding Author Emails: r.j.foster00@leeds.ac.uk p.j.hine@leeds.ac.uk i.m.ward@leeds.ac.uk

1 Introduction

Nanoscale fillers offer the potential for significant enhancement of a range of polymer properties, as they are available in a wide variety of shapes and properties. Carbon nanotubes (CNT) and nanofibres (CNF) have been used extensively in the literature, yet very few analytical studies of the material properties have been reported. Here we use the Cox-Krenchel model to interpret the experimentally measured changes in Young's modulus from particle aspect ratio reduction during to processing, in addition to the measurement of the mechanical properties of the composite.

Hot Compaction, a process developed at the University of Leeds [1], utilises high modulus, highly oriented elements to form thick section, homogeneous sheets without the need to introduce a second phase of different chemical composition. These 'single polymer' composites are produced by selective melting on the surface of the oriented elements; on cooling, this molten material re-crystallises to form a matrix phase and bind the oriented elements together. CNF filled polypropylene (PP) tapes have been produced and successfully hot compacted into sheets. The properties of these nanofilled self-reinforced single polymer composites is reported. Of particular interest has been to investigate the introduction of interleaved films, an extension of recent work conducted by two of this papers authors [2] of the same polymer or nanocomposite in order to establish the change in properties when the CNF are incorporated in the drawn tapes, in the interleaved films or both.

2 Experimental

2.1 Materials

The polypropylene (PP) used in this work was a homopolymer with a weight average molecular weight (M_W) of 360,000 and a density of 910kgm^{-3} [3]. The Carbon Nanofibres (CNF) used were obtained from Pyrograf Products Inc, a division of Applied Sciences Inc, Cedarville, OH. These CNF are vapour grown CNF, and are pyrolytically stripped fibres, which removes polyaromatic hydrocarbons from the surface of the fibres [4], which were received in a powder-like "soot" form. The as-received fibres are shown in figure 2.

2.2 Processing

2.2.1 Blending and production of nanocomposite sheets

Blending of the CNF into the PP was achieved using a Thermo Electron Corporation twin-screw extruder. Using previous work as a guideline [3, 5], a loading of 10% by

weight (%*w/w*) (5% by volume) of CNF was used. Blending was done both at extruder temperatures of 200 and 230°C, and at a screw speed of ~70*rpm*. The twin screw extruder was set up with three mixing zones along the length of the extruder barrel, and the PP/CNF material passed through the extruder up to three times, meaning nanocomposite material was produced that had been passed through one, four or seven mixing zones (the CNF was first introduced into the extruder before the final mixing zone). The extruded material was quenched and pelletised.

Compression moulded sheets were produced for tensile tests from the pelletised material in a hot press set to 210°C, and at a nominal pressure of 0.7*MPa* for 3 minutes. The pressure on the sheet was then increased to a maximum of 10*MPa* at 210°C for 10 seconds, before rapid quenching at pressure.

As shown in section 4.2.1, the optimum blending conditions were determined to be passing the material through 4 mixing zones at 200°C. All material for hot compaction was produced with this blending regime. Material was also produced with 2% Maleic Anhydride grafted PP by weight blended into the material and subsequently blended with CNF with the same regime.

2.2.2 Extrusion of blown films

PP, PP/CNF and compatibilised PP/CNF were processed into a blown film using a small-scale blown film line at Bradford University. The material was blown into a film by passing the material from an extruder through an annular die. The blown film then travelled through air for ~0.5*m* to allow cooling to room temperature before haul-off. The processing conditions were chosen to produce the thinnest film possible.

2.2.3 Production of woven hot compacted sheets

The optimally blended PP/CNF material was melt-spun and drawn into tapes along with unmodified PP melt-spun and drawn tapes on a continuous drawing frame. Both were drawn to a draw ratio of ~11. The tapes were then woven into cloths and subsequently hot compacted into sheets at a compaction temperature of 187°C. Samples were also produced with interleaved film layers in between the woven tape layers. All compacted samples produced were 8ply and had a thin layer of aluminium foil introduced along one edge of the compacted sample in order to act as a starting crack for the T-Peel tests.

2.3 Mechanical testing

2.3.1 Tensile Young's modulus testing

The tensile mechanical properties of the isotropic compression moulded sheets and hot compacted sheets were investigated using an RDP-Howden servo-mechanical tensile testing machine and videoextensometer. All tensile tests were performed at a nominal strain rate of $5x10^{-3}\ s^{-1}$, a temperature of 21±1°C and a relative humidity of 50%. The Young's modulus was taken as the initial modulus (<1% strain) from the stress strain curve.

2.3.2 T-Peel testing

T-Peel tests were performed on an RDP-Howden servo-mechanical tensile testing machine, using the aluminium foil introduced during the hot compaction process as a starting crack. All samples were 10*mm* wide and ~80*mm* long. The tests were performed at a rate of 80 *mm/min*, temperature of 21±1°C and relative humidity of 50%. The force output from the testing machine during each test was recorded, and the peel force/10*mm* was determined as the average force during the test. Small samples of the peel surface

were cut directly from the samples for observation in a scanning electron microscope (SEM) (for procedure see the later section).

2.4 Fibre aspect ratio measurement

2.4.1 Scanning electron microscopy (SEM)

2.4.1.1 Ashing of composite

The blended PP/CNF composite material from each stage of mixing (1, 4 and 7 mixing zones) was vaporized at 400°C for two and a half hours to remove all PP, leaving only the CNF. The residue was then dispersed in a water/surfactant solution and placed on an SEM stub for observation. These were compared to the as-received CNF. All samples were sputter-coated with platinum (~3*nm* thick) in argon plasma and observed in a LEO1530 FEGSEM.

2.4.1.2 Nanocomposite fracture surfaces

The CNF were examined in-situ in the PP/CNF nanocomposite by observing 'freeze fracture' samples produced from the composite compression moulded sheets. Small samples were cut from the sheet, immersed in liquid nitrogen for ~30s, and fractured. The samples were then mounted on the SEM stub, such that the fracture surface of the sample was observed, coated in with silver paint down one side to improve conductivity, and sputter-coated in the same fashion described above.

2.4.1.3 CNF diameter measurement

The diameter of the CNF was determined by using a simple image analysis tool (UTHSCSA Image Tool 3.0), to measure the average diameter of 220 fibres from SEM images of as-received CNF, ashed CNF residue and CNF in-situ in the nanocomposite.

2.4.2 Dynamic light scattering (DLS)

PP/CNF nanocomposite blended pellets were refluxed in boiling Xylene for 20 minutes in order to dissolve all PP from the nanocomposite. The solution was then filtered in through a sintered glass filter, leaving the CNF on the filter. The CNF filtrand was then dispersed in a water/surfactant solution (1% *w/w*). This solution was then further diluted to ~10^{-3}%*w/w* CNF, as detailed by Badaire et al [6]. The autocorrelation functions from dynamic light scattering experiments conducted at a scattering angle of 30° was then fitted using the model detailed in Badaire et al [6], to determine the CNF length.

3 Analytical Models

Analytical models have been used to investigate the structure-property relationship of the stiffness of the PP/CNF material produced in this work. The experimentally determined results have been compared to the Cox-Krenchel model [7, 8].

The stiffness of the hot compacted sheets has been modelled using the laminate model, a modification of the rule of mixtures, using differential scanning calorimetry (DSC) to determine the amount of material in each of the oriented and isotropic phases.

3.1 Cox-Krenchel model

The Cox-Krenchel model, developed initially by Cox [8], and further refined by Krenchel [7], is a modification of the rule of mixtures to describe the composite Young's modulus (E_C) accounting for fibre length and fibre orientation [9]. This is described by equation (1):

$$E_C = \eta_o \eta_l V_f E_f + V_m E_m \qquad (1)$$

Where the subscripts *c*, *f* and *m* refer to the composite, reinforcing fibre and matrix respectively, and *E* is the Young's modulus, *V* is the volume fraction and η_o and η_l are the orientation and length efficiency factors as given by equations (2) and (3)

$$\eta_l = 1 - \frac{\tanh(\beta l/2)}{(\beta l/2)} \tag{2}$$

Where l is the fibre length, and β is given by:

$$\beta = \left(\frac{2\pi G_m}{E_f A_f \log_e(R/r)} \right)^{\frac{1}{2}}$$

Here, *G* is the shear modulus, *A* is the fibre cross-sectional area, *r* is the fibre diameter and *R* is fibre separation.

$$\eta_o = \left\langle \cos^4 \theta \right\rangle \tag{3}$$

Where the fibre direction is described by the angle, θ. For continuous fibre distributions, equation (3) is integrated over all angles, giving a $\eta_o = 1/5$ for a random 3D distribution of fibres and $\eta_o = 3/8$ for a random 2D fibre distribution.

3.2 Laminate model

The laminate model is another extension of the rule of mixtures model, simply allowing for the fact that the woven hot compacted sheets are composed of woven tapes, aligned both parallel and transverse to the loading direction (in-plane), and of an isotropic phase produced from the compaction process (melting of the tapes) and from the interleaved films. The composite modulus can thus be determined from equation (4) using measurement of the longitudinal Young's modulus of the woven tapes and of the isotropic phase. DSC was used to determine the amount of material in each phase and the transverse modulus of the tapes was assumed to be equal to the isotropic phase.

$$E_C = \left(\frac{V_{Tape}}{2} \right) E_{Tape} + \left(1 - \frac{V_{Tape}}{2} \right) E_{Isotropic} \tag{4}$$

4 Results

4.2 Isotropic PP/CNF nanocomposite material

4.2.1 Tensile Young's modulus

The tensile Young's modulus of the blended PP/CNF nanocomposite material blended by 1, 4 and 7 mixing zones (1, 2 and 3 extrusions) is shown in Figure 1.

Figure 1 shows that the there is a clear peak in the Young's modulus, (2.12±0.09)*GPa* after the material has passed through 4 mixing zones (2nd extrusion). The increase in Young's modulus, over the material blended by a single mixing zone, is attributed to increased dispersion of the CNF in the polypropylene matrix. The subsequent decrease in modulus in the material blended by seven mixing zones is attributed to a shortening of the CNF due to the high shear process, which leads to a reduction in the reinforcing efficiency. The comparative results of the pure PP processed in the same fashion as the PP/CNF nanocomposite show that incorporation of CNF leads to improved stiffness.

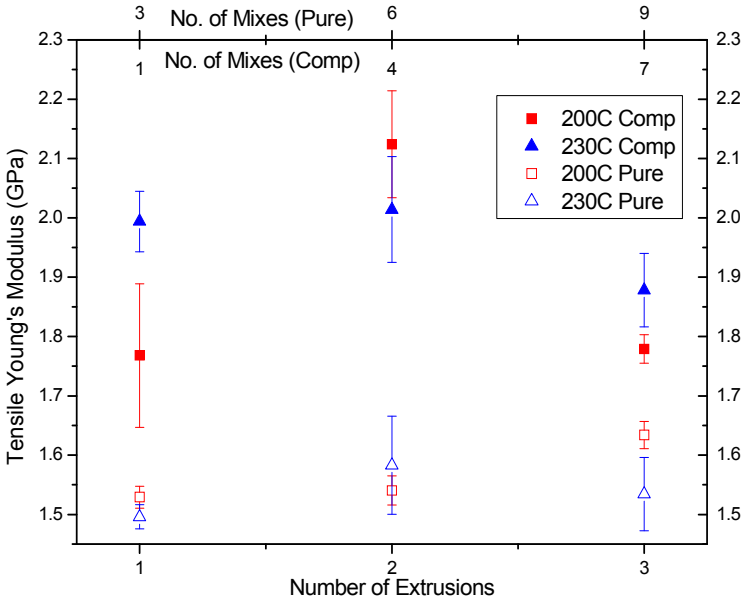

Figure 1 Young's modulus of Compression-Moulded Sheets obtained from static tensile testing. The filled symbols (■▲) represent the 10% w/w Carbon Nanofibre/Polypropylene composite sheets and the open symbols (□△) represent pure polypropylene sheets. The ■□ points were blended at 200°C and ▲△ points at 230°C

4.2.2 Fibre dispersion (SEM analysis)

Comparison of the ashed composite residue provided important information on the dispersion of the CNF throughout the composite, particularly with reference to the as-received fibres (figure 2). Figure 3 shows the residue of the ashed composite residue from the material blended by a single mixing zone. The ball-like aggregates of CNF, similar in size to the as-received CNF, are a clear indication that the single mixing zone is insufficient to break up the as-received CNF balls. Analysis of the material blended through 4 and 7 mixing zones showed large matted aggregates of CNF, much larger than the balls of as-received fibres, indicating good dispersion. These matted aggregates were formed during the vaporization process.

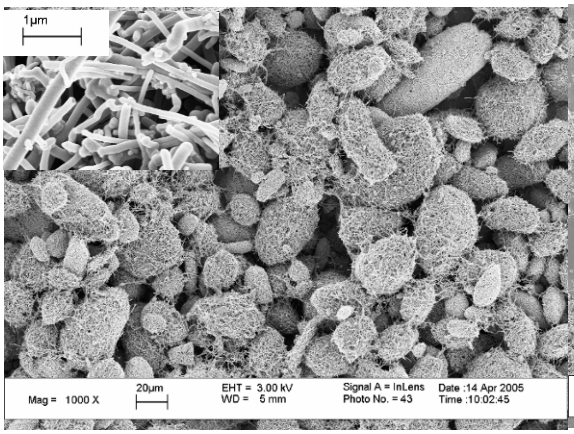

Figure 2 SEM image of as-received CNFs. The size of the balls proved to be a good indication how the extrusion process broke up the CNF assembly. The scale bar indicates 20µm. The inset shows a higher magnification of the CNF

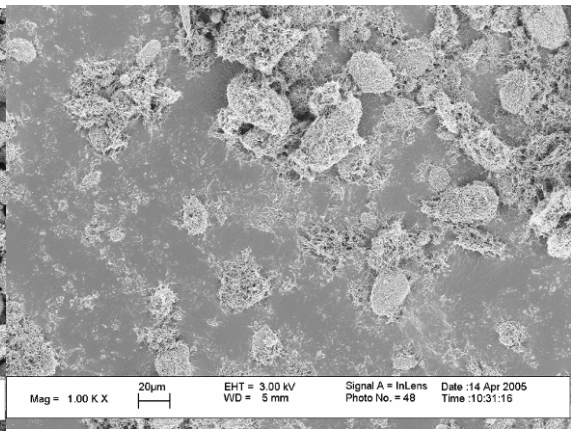

Figure 3 Residue from ashed composite mixed at 200°C and one extrusion (one mixing zone). Although a large number of balls are still visible, the majority have begun to be broken up. The scale bar is 20µm.

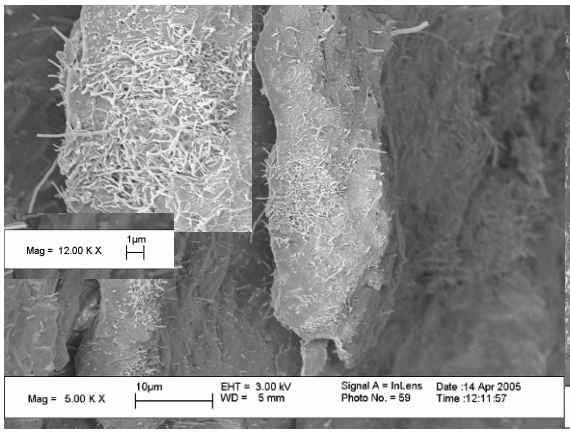

Figure 4 Freeze fracture of PP/CNF sheet produced with material blended through one mixing zone at 200°C. The inset (scale 1μm) shows a large unwetted region of fibres. The scale on the main image is 10μm.

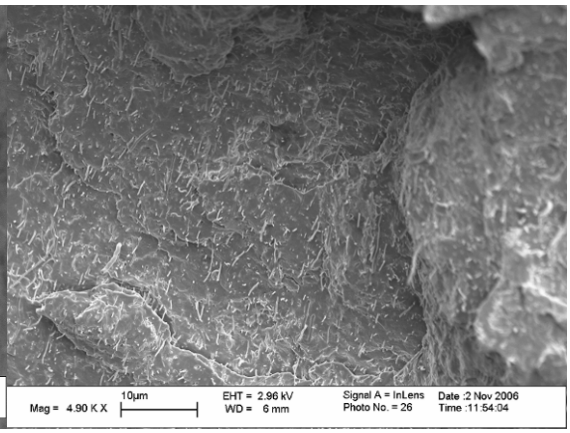

Figure 5 Freeze fracture of PP/CNF sheet produced with material blended through four mixing zones at 200°C. An even dispersion of CNF is seen throughout the composite. The scale on the main image is 10μm.

The improved dispersion of CNF throughout the nanocomposite as the material is blended through four and seven mixing zones is shown in Figures 4 and 5. Figure 4 shows the large unwetted regions of CNF visible throughout the nanocomposite, again indicating that the 'ball-like' as-received CNF assemblies have not been broken up and dispersed in the PP. Figure 5 shows that after four mixing zones, the as-received CNF 'balls' have been completely broken up and the CNF are spread throughout the PP matrix. A similar dispersion was seen in the material that had been blended through 7 mixing zones.

4.2.3 Measurement of fibre aspect ratio

The post-blending CNF length was determined from fitting the DLS autocorrelation function using the model as proposed by Badaire et al [6]. The results from this fit are shown in Table 1. The CNF diameter was measured from image analysis of SEM images of the CNF. The distribution of the measured 220 fibre diameters is shown in figure 6, binned into 20*nm* groups. The fibre aspect ratio was then determined from these measurements. Measurement of the fibre length for the material that was blended by a single mixing zone was not possible since the fibres were still highly aggregated.

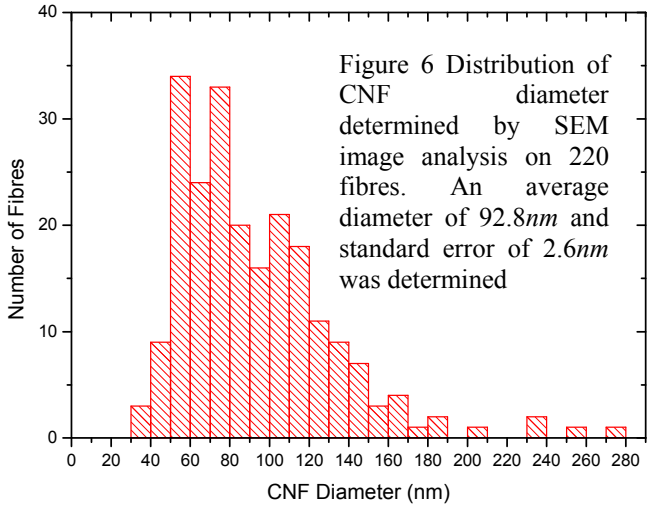

Figure 6 Distribution of CNF diameter determined by SEM image analysis on 220 fibres. An average diameter of 92.8*nm* and standard error of 2.6*nm* was determined

Table 1 CNF fibre lengths as determined from DLS autocorrelation functions fitted by the function in ref [6]. The errors were determined from the error in the function fit.

No. of Mixing Zones	4	7
Fitted length from DLS autocorrelation function (μm)	3.175±0.001	2.66±0.03
CNF aspect Ratio	34±1	28.7±0.8

4.2.4 Analytical modelling

The comparison between the experimentally measured Young's modulus and that predicted by the Cox-Krenchel and Aggregate models is shown in Table 2. The Cox-Krenchel model is seen to overestimate the nanocomposite modulus for both the material blended through four and seven mixing zones. A possible explanation for this is limited aggregation of the CNF within the composite, where instead of isolated CNF reinforcing the PP matrix, two fibres (on average) touching side-by-side are aggregated. Using the Cox-Krenchel model (3D orientation) with this proposed aggregation predicts moduli of (2.04±0.04)*GPa* for 4 mixing zones and (1.90±0.03)*GPa* for 7 mixing zones, which are within the error of the experimental measurements.

4.3 Hot Compacted nanocomposite material

4.3.1 Tensile Young's modulus

The tensile Young's moduli for the various combinations of pure and nanocomposite woven tapes and films compacted in this work are shown in table 3. As expected, the nanocomposite compacted sheets show an improved Young's modulus over the comparable pure PP compacted sheets. Also, as expected, the introduction of film gives an increase in the isotropic phase material, leading to a reduction in the tensile Young's modulus of the hot compacted composite sheets. This effect was reported by some of the authors in pure PP commercially woven cloths with interleaved PP films [2, 10]. Interestingly, incorporation of the CNF into both the tapes and the interleaved films resulted in a Young's modulus comparable to that of the standard PP compaction. The introduction of the Maleic Anhydride grafted PP had no effect on the Young's modulus of the composite hot compacted sheets.

4.3.2 Laminate modelling

Differential scanning calorimetry (DSC) was used to determine the amount of material in each of the oriented and isotropic phases of the woven hot compacted sheets shown in table 3. The tensile Young's modulus of isotropic PP and PP/CNF material and the drawn PP and PP/CNF tapes was determined by the same method described in section 2.3.1. Equation (4) was then used to predict the composite Young's modulus and compared to the experimentally determined modulus, as shown in table 3.

Table 2. Comparison of Experimentally determined Young's modulus of the PP/CNF nanocomposite material (blended by 4 and 7 mixing zones) with the Cox-Krenchel model predictions of composite stiffness, determined from the measured fibre aspect ratios.

	Young's Modulus (GPa)	
No. of Mixes	4	7
Experimentally Measured (200°C blending temp)	2.1±0.2	1.78±0.06
2D fibre orientation	3.80±0.04	3.46±0.05
3D fibre orientation	2.71±0.03	2.53±0.02
3D fibre orientation (aggregated fibres)	2.04±0.04	1.90±0.03

In general all composite modulus predictions given by the laminate model, equation (4), are within the error of the experimentally determined moduli, showing that a simple two phase model gives good predictions from the properties of the two phases for the woven hot compacted sheets.

4.3.3 T-Peel tests

The peel load required to propagate a crack between the layers of the woven hot compacted sheets for the samples produced in this study are shown in Figure 7, and in Table 3. From figure 7, there are four clear populations of compacted sample peel load, that of pure PP, PP/CNF nanocomposite, pure PP woven tapes with PP film and the compacted samples with nanocomposite in either the woven tapes, interleaved film or both. These results indicate that it is the CNF at the interface in the melted and recrystallised material produced in the hot compaction process that are important in improving the crack resistance between the woven layers. From these results, it can be concluded that incorporation of the CNF increases the peel load of the compacted samples; a film layer further improves the peel load and the incorporation of the CNF to the film samples results in a further improvement. In addition, the results indicate that there is no difference if the CNF are incorporated into the tape, the film or both, suggesting that it important that the CNF are located at the interface region between fibre and tape, through which the crack propagates. Interestingly, as shown in Table 3, introduction of the Maleic Anhydride grafted PP compatibiliser has no effect on the peel load of the woven compacted nanocomposite material.

4.3.4 SEM of peel surfaces

SEM images of the peel surfaces, as shown in Figure 8, show a similar trend to the peel results in Figure 7. The surface of a pure PP sample, shown in Figure 8 (a) shows little damage across the surface. Incorporation of the CNF to the compacted sheet (figure 8 (b)) results in greater damage across the surface, and signs of fibrillation can be seen down the right hand side of the image. Figure 8 (c) (PP sample with PP interleaved film) shows a huge amount of fibrillation across the entire surface, resulting in the increased peel load. Finally, Figure 8 9(d) shows a huge amount of damage, including tape pull-out from the surface when the CNF are incorporated.

Table 3. Tensile Young's modulus and peel loads of woven hot compacted sheets for PP and PP/CNF composites, with and without interleaved films. The laminate modulus predictions are shown as a comparison.

System		Compaction Temp (ºC)	Young's Modulus (*GPa*)		Peel Load (*N*/10*mm*)
Tape	Film		Expt	Laminate Model	
PP	None	187.3	3.2±0.2	3.3±0.4	0.28±0.02
PP	None	188.6	2.7±0.1	3.2±0.3	0.46±0.04
PP/CNF	None	187.6	3.8±0.5	2.8±0.3	4.6±0.7
PP/CNF	None	188.7	4.3±0.5	3.8±0.3	5.1±0.7
PP	PP	187.8	2.3±0.2	3.5±0.2	11.3±0.5
PP	PP/CNF	187.8	2.5±0.3	2.6±0.1	19±3
PP/CNF	PP	187.7	2.3±0.2	3.0±0.2	16±2
PP/CNF	PP/CNF	187.6	3.0±0.2	3.0±0.2	19±2
PP	PP/CNF/MaH	187.9	2.1±0.3	----	18.4±0.5
PP/CNF	PP/CNF/MaH	188.1	2.6±0.1	----	17.5±0.5

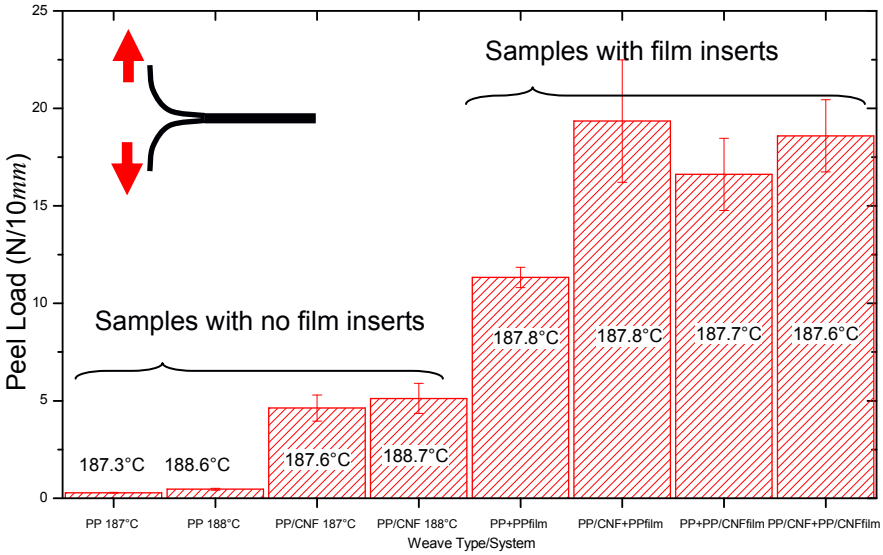

Figure 7. Peel Loads of woven hot compacted samples with and without interleaved film inserts. The samples shown (L-R) are two PP and two PP/CNF without interleaved films, PP tapes with PP film, PP tapes with PP/CNF film, PP tapes with PP/CNF film and PP/CNF tapes with PP/CNF film. The compaction temperatures are shown

5 Conclusions

The optimum blending conditions of CNF into PP, at a loading of 10%*w/w*, using a twin screw extruder has been determined, by measurement of the Young's modulus of the resultant nanocomposite. The variation in Young's modulus with blending has been linked firstly to an improvement in CNF dispersion (determined by SEM), followed by reduction in particle aspect ratio.

A combination of SEM image analysis and dynamic light scattering has been used to quantitatively determine the changes in CNF aspect ratio due to the blending process. The Cox-Krenchel model has been used to give an insight into the structure-property relationship of the nanocomposite material; however further analysis and modelling is required to fully understand the processing-structure-property relationship.

The tensile Young's modulus of the hot compacted nanocomposite material has been determined and modelled successfully using the laminate model. Crucially, the peel strength of the hot compacted composites has been shown to be improved significantly by the incorporation of the CNF.

Further improvement has been found by using interleaved films, with incorporated CNF. Most interestingly, it has been shown that the improvement in the peel load of the hot compacted sheets with interleaved films is independent of the whether the CNF are incorporated into the woven tape layers, the film layers or both. This result suggests that the properties of the interface between the tapes and isotropic matrix are controlling the fracture of the sample.

Further investigation is currently ongoing to understand the full process taking place during the crack propagation, although the measured peel load has been correlated to the surface damage observed in SEM samples.

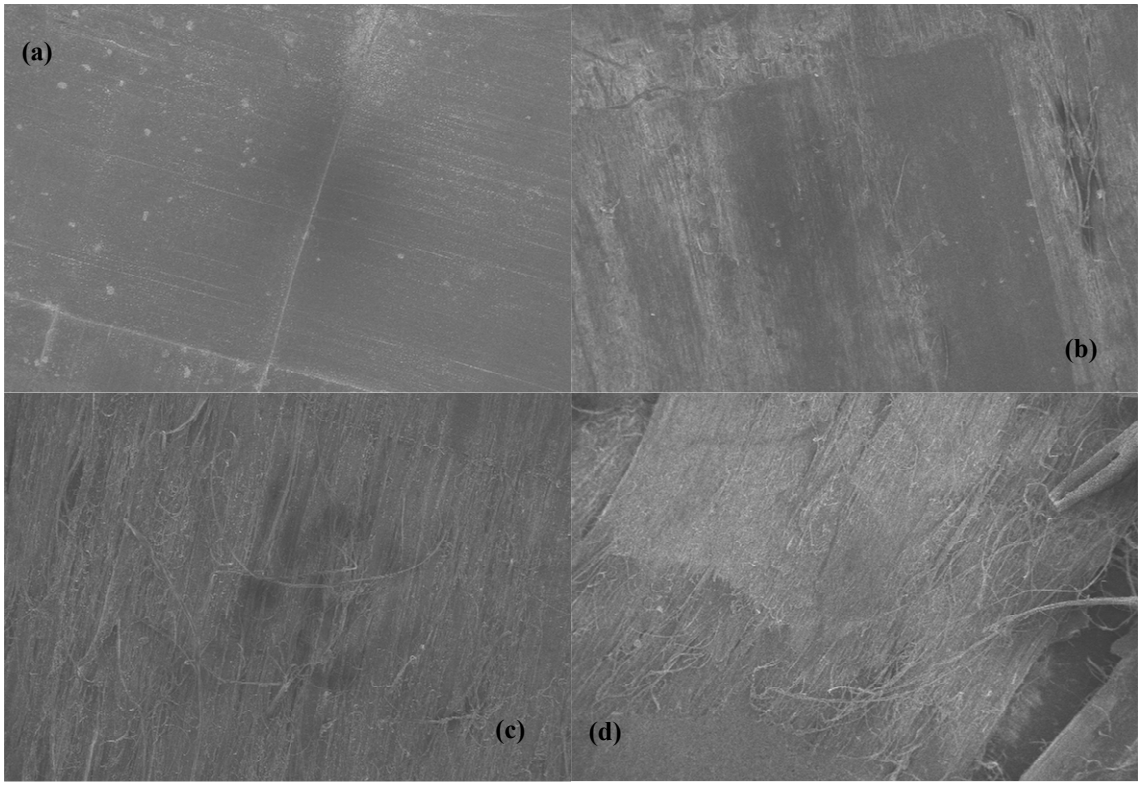

Figure 8. Peel surfaces of compacted sheets observed under SEM of (a) PP (no film), (b) PP/CNF (no film), (c) PP with PP film and (d) PP with PP/CNF film. The amount of damage is clearly seen to increase on the surface of the peel sample, corresponding to the increase in peel load observed.

Acknowledgements

We thank the University of Leeds Nanomanufacturing Institute (NMi) for funding this research. We would also like to thank Manlio Tassieri and Dr Tom Waigh for their help and expertise with Dynamic Light Scattering.

References

1. Ward, I. M., Hine, P. J., "The science and technology of hot compaction", *Polymer*, 2004; 45, 1423-1437.
2. Hine, P. J., *et al.*, "The use of interleaved films for optimising the production and properties of hot compacted, self reinforced polymer composites", *Composites Science and Technology*, 2008; 68, 1413.
3. Hine, P., *et al.*, "The incorporation of carbon nanofibres to enhance the properties of self reinforced, single polymer composites", *Polymer*, 2005; 46, 10936-10944.
4. *Pyrograf Products Incorporated: Pyrograf III*. 16th July 2007. Available from: http://www.apsci.com/ppi-pyro3.html.
5. Foster, R. J., *et al.*, "The Incorporation of Nanoscale Particles to Enhance the Properties of Oriented Polymers", *ECCM12*, Biarritz, France, 2006.
6. Badaire, S., *et al.*, "In situ measurements of nanotube dimensions in suspensions by depolarized dynamic light scattering", *Langmuir*, 2004; 20, 10367-10370.
7. Krenchel, H., "Fibre Reinforcement", *Akademisk Forlag*, 1964.
8. Cox, H. L., "The elasticity and strength of paper and other fibrous materials", *British Journal of Applied Physics*, 1952; 3, 72-79.
9. Folkes, M. J., "Short Fibre Reinforced Thermoplastics", Research Studies Press, Division of John Wiley & Sons, 1985.
10. Hine, P. J., *et al.*, "The Use of Interleaved Films for Optimising the Production and Properties of Hot Compacted, Self Reinforced Polymer Composites", *ECCM12*, Biarritz, France, 2006.